SESAM mode-locked red praseodymium laser

Maxim Gaponenko,[1,*] Philip Werner Metz,[2] Antti Härkönen,[3] Alexander Heuer,[2,4] Tomi Leinonen,[3] Mircea Guina,[3,5] Thomas Südmeyer,[1] Günter Huber,[2,4] and Christian Kränkel[2,4]

[1]*Laboratoire Temps-Fréquence, Université de Neuchâtel, Neuchâtel 2000, Switzerland*

[2]*Institut für Laser-Physik, Universität Hamburg, Hamburg 22761, Germany*

[3]*Optoelectronics Research Centre, Tampere University of Technology, Tampere 33720, Finland*

[4]*The Hamburg Centre for Ultrafast Imaging, Universität Hamburg, Hamburg 22761, Germany*

[5]*RefleKron Ltd., Tampere 33800, Finland*

**Corresponding author: maxim.gaponenko@unine.ch*

Received October 9, 2014; revised November 4, 2014; accepted November 12, 2014; posted November 14, 2014 (Doc. ID 224598); published December 12, 2014

We present the first semiconductor saturable absorber mirror (SESAM) mode-locked praseodymium solid-state laser. The laser is based on a Pr^{3+}:$LiYF_4$ crystal as gain medium and a GaInP-quantum well-based SESAM. Self-starting continuous-wave mode-locked laser operation with an average output power of 16 mW is achieved at a center wavelength of 639.5 nm. The laser operates at a repetition rate of ~85.55 MHz and emits pulses with a duration of ~18 ps.

OCIS codes: (140.3580) Lasers, solid-state; (140.4050) Mode-locked lasers; (140.7300) Visible lasers.

http://dx.doi.org/10.1364/OL.39.006939

Coherent light sources emitting in the visible spectral range attract much attention not only due to their numerous applications in entertainment and education, but also due to their potential for biomedical applications such as multicolor flow cytometry or confocal fluorescence microscopy with high spatial resolution [1,2]. Trivalent praseodymium (Pr^{3+}) as an active ion in bulk or waveguide laser geometry is one of the best candidates for efficient visible solid-state lasers [3–11]. In continuous-wave operation, bulk Pr lasers achieve output powers up to 4 W in the green (~520 nm) [4], 3 W in the red (~640 nm) [5], and 2 W in the orange (~600 nm) [5] spectral regions with optical-to-optical efficiencies exceeding 40%. In these cases, the pump sources were intracavity frequency-doubled optically pumped InGaAs semiconductor disk lasers (2ω-OPSL) at 480 nm. The ongoing development of blue InGaN laser diodes with emission wavelengths around 445 nm also enables efficient directly diode-pumped Pr^{3+} lasers [10,11].

So far, there are only a few reports on the realization of mode-locked Pr^{3+}-lasers. A dye-laser pumped Pr^{3+}-doped fiber laser was mode-locked by use of an external cavity with a vibrating mirror [12]. It generated 44-ps pulses at a repetition rate of 96 MHz with an average output power of 40 mW at 1048 nm [12]. The only mode-locked visible Pr^{3+}-laser so far was reported in 1995 by Ruan *et al.* [13]. Their crystalline solid-state Pr^{3+}:$LiYF_4$ laser used Kerr-lens mode-locking (KLM) and was pumped by an argon–ion gas laser. In addition, a CdSeS-colored glass or dye saturable absorber was required to start the KLM operation. An average output power of 30 mW and 8-ps pulses at a repetition rate of 125 MHz were generated at a wavelength of 639 nm [13]. At a wavelength of 607 nm, the laser emitted 10-ps pulses at a repetition rate of 100 MHz with an average output power of 24 mW [13]. Tong *et al.* [14] reported later on the optimized cavity configuration of such a laser, which allowed achieving the KLM operation initiated by a mechanical perturbation (tap starting). With two prisms used for dispersion compensation inside the cavity, the laser produced 15-ps pulses at a repetition rate of 70 MHz with an average output power of 15 mW at 607 nm [14]. Employing the vibrationally broadened optical transition at 613 nm, the same group demonstrated later generation of 400-fs pulses. The pulse duration was limited by the gain bandwidth. However, to initiate the KLM operation, placement of a cavity end mirror on a continuously vibrating assembly was required [15]. Abe *et al.* [16] reported on the use of Cr^{4+}:YAG and CdSeS-colored glass saturable absorbers in a diode-pumped 639-nm Pr^{3+}:$LiYF_4$ laser. However, only a Q-switched mode-locked operation was achieved. Recently, semiconductor saturable absorber mirrors (SESAMs) based on GaInP quantum wells were introduced for passive mode-locking of red OPSLs emitting at wavelengths of 675 nm [17] and 664 nm [18], which are also highly attractive for mode-locking of other laser types. Here, we report, to the best of our knowledge, the first SESAM mode-locked Pr^{3+}-laser. It is pumped at 480 nm by a 2ω-OPSL. The pulse formation is fully self-starting.

The 1.75-m long laser cavity is formed by three concave mirrors M1, M2, M3 ($r_{M1} = 50$ mm, $r_{M2} = r_{M3} = 100$ mm), and one plane mirror M4 [Fig. 1(a)]. We use a Pr^{3+}(0.2 at.%):$LiYF_4$ crystal with a thickness of 2 mm as a gain medium. The laser crystal is mounted on a water-cooled copper heat sink. It is placed between the concave mirrors, M1 and M2, at Brewster's angle for light polarized parallel to the a-axis of the crystal. The intracavity mode radius in the gain medium was calculated to be $\sim 50 \times 70\ \mu m^2$. The output coupler M1 has a transmission of $T = 1\%$ at the laser wavelength of 640 nm, while all other cavity mirrors are highly reflective for this wavelength. A 2ω-OPSL is used as pump source. It provides 3.75 W of pump power incident on the gain medium at a wavelength of 480 nm. The pump beam with an $M^2 < 3$ is focused to a beam waist with a radius of ~50 μm inside the gain medium. The pump beam was polarized parallel to the c-axis of the laser crystal to account for the higher absorption cross-sections in this orientation. This led, however, to Fresnel losses of the pump at the input facet of the gain medium. An output

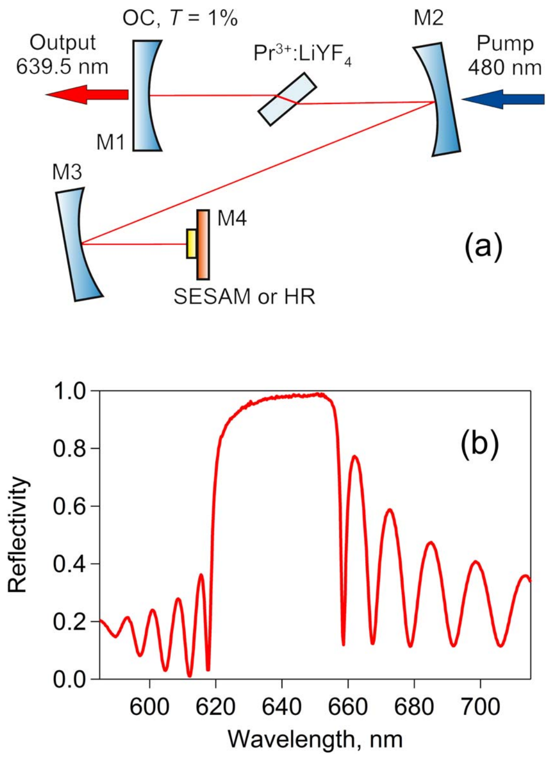

Fig. 1. Cavity configuration of the mode-locked Pr^{3+} : $LiYF_4$ laser (a) and the reflectivity spectrum of the GaInP SESAM (b).

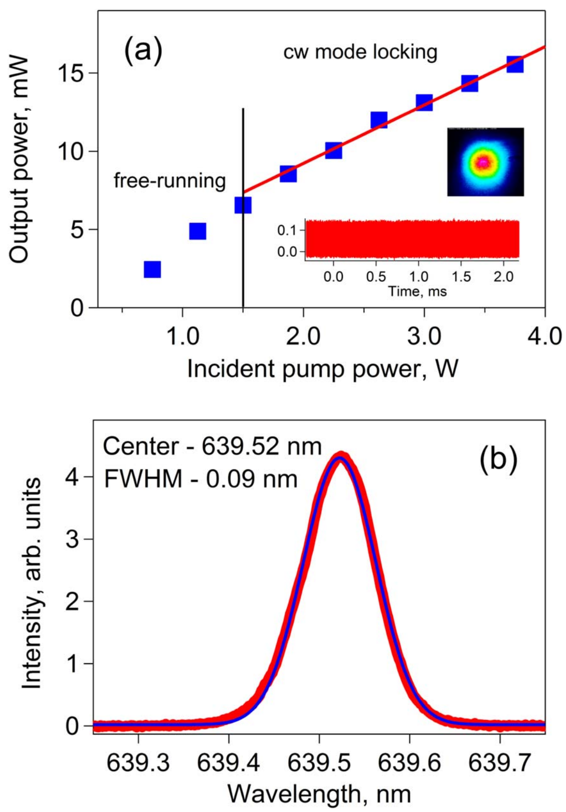

Fig. 2. (a) Output power of the Pr^{3+}:$LiYF_4$ laser versus the incident pump power. The insets show the output-beam profile and the pulse train in a millisecond time scale. (b) Optical spectrum of the mode-locked Pr^{3+}:$LiYF_4$ laser measured at the maximum output power with a spectral resolution of 0.02 nm. The red line represents the experimental data; the blue line is a Gaussian fit.

power of 370 mW was achieved in free-running cw Pr^{3+}-laser operation.

For achieving mode-locking, we replaced the plane mirror M4 by a SESAM. The SESAM contains three GaInP quantum wells with 6-nm thickness each, embedded within an AlGaInP cavity, and placed on top of a 40-pair AlGaAs/AlAs DBR. The structure exhibits an unsaturated reflection of 97% at the laser wavelength [Fig. 1(b)]. Data on the nonlinear parameters of the SESAM such as modulation depth, saturation fluence, and absorption recovery time are currently not available. The SESAM is mounted on a copper heat sink. The mode radius on the SESAM was calculated to be ~25 μm.

At a threshold of 1.5 W of incident pump power, the laser switches to stable self-starting continuous-wave mode-locked operation [Fig. 2(a)]. The laser operates in fundamental TEM_{00} mode with a maximum output power of 16 mW at an incident pump power of 3.75 W [Fig. 2(a)].

The laser operates stably over several days without changes of the output characteristics. The optical spectrum [Fig. 2(b)] is centered at a wavelength of 639.52 nm and is well approximated with a Gaussian fitting function with a full width at half-maximum (FWHM) of 0.09 nm, supporting ~5 ps transform-limited pulse duration (assuming sech^2 temporal profile). The radio-frequency spectrum of the laser output ([Fig. 3]) shows the absence of parasitic side peaks and indicates a stable single-pulse mode-locking operation. The pulse repetition rate is ~85.55 MHz [Fig. 3(b)]. Single-pulse laser operation is

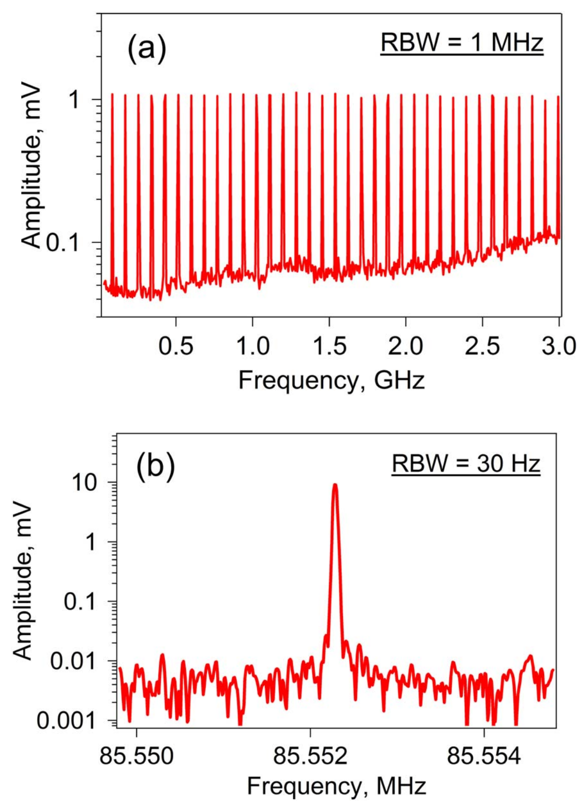

Fig. 3. Radio-frequency spectrum of the mode-locked Pr^{3+}:$LiYF_4$ laser measured with a 25-GHz fast photodiode using a 3-GHz span at 1-MHz resolution bandwidth (a) and a 5-kHz span at 30-Hz resolution bandwidth (b).

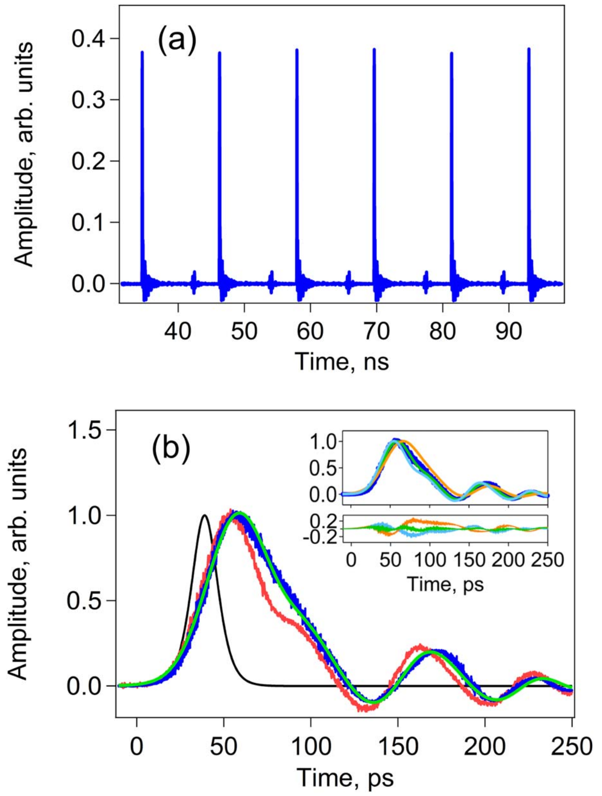

Fig. 4. Pulse train of the passively mode-locked $Pr^{3+}:LiYF_4$ laser (a) and the single-pulse trace (b) measured with a fast photodiode and a sampling oscilloscope. Green line in (b) represents a fit of the measured data (blue) by a convolution of the detection-system temporal response (red) with an 18-ps FWHM $sech^2$-shape laser pulse (black). Inset in (b) represents, for reference, convolutions of the detection system temporal response with 30-ps (orange), 18-ps (green), and 10-ps (light blue) FWHM $sech^2$-shape laser pulses. Corresponding residuals of the fittings are presented in the bottom part of the inset.

further confirmed by analyzing the pulse train with a 35-GHz-bandwidth sampling oscilloscope and a 25-GHz photodiode [Fig. 4(a)]. The same equipment was used to measure the laser pulse duration [Fig. 4(b)]. The temporal response function of the detection system was determined in an independent experiment using 3-ps pulses at 980 nm. The measured mode-locked Pr-laser pulse traces with a FWHM of 50 ps were fitted by a convolution of the detection-system response function and a $sech^2$-shape pulse. The width of this $sech^2$-pulse was used as a fitting parameter. The results are presented in Fig. 4(b). The estimated pulse duration of the mode-locked Pr^{3+}-laser is FWHM = 18 ps.

Future improvements will require an implementation of intracavity dispersion compensation by means of a prism pair or dispersive mirrors, and a detailed investigation of the nonlinear spectroscopic parameters of the GaInP SESAMs, which should allow for an optimization of the laser design and its output characteristics. The 639-nm emission peak in $Pr^{3+-}:LiYF_4$ has a FWHM of ~0.8 nm, which should support sub-ps pulse durations. Moreover, GaInP SESAMs can also be engineered for operation at shorter wavelengths. This is particularly interesting due to the presence of a wide emission band in $Pr^{3+}:LiYF_4$ crystals at a wavelength around 620 nm. In our experiments we were able to achieve continuously tunable diode-pumped cw operation in the wavelength range of 618–622 nm with an average output power of 100 mW. The optical bandwidth of this laser transition should therefore allow for mode-locked solid-state Pr^{3+}-lasers with <200 fs pulse duration.

In summary, we present the first SESAM mode-locked Pr^{3+}-laser. The laser operates at a wavelength of 639.52 nm and delivers 18-ps pulses with an average power of 16 mW. Our result is the first step toward efficient and powerful direct visible femtosecond diode-pumped solid-state lasers, which should be achievable given the excellent properties of Pr^{3+}-doped gain materials and the design flexibility of the SESAM-mode-locking technology.

References

1. N. Baumgarth and M. Roederer, J. Immunol. Methods **243**, 77 (2000).
2. J.-A. Conchello and J. W. Lichtman, Nat. Methods **2**, 920 (2005).
3. A. Richter, N. Pavel, E. Heumann, G. Huber, D. Parisi, A. Toncelli, M. Tonelli, A. Diening, and W. Seelert, Opt. Express **14**, 3282 (2006).
4. V. Ostoumov and W. Seelert, Proc. SPIE **6871**, 68711K (2008).
5. P. W. Metz, F. Reichert, F. Moglia, S. Müller, D.-T. Marzahl, C. Kränkel, and G. Huber, Opt. Lett. **39**, 3193 (2014).
6. F. Reichert, D.-T. Marzahl, P. Metz, M. Fechner, N.-O. Hansen, and G. Huber, Opt. Lett. **37**, 4889 (2012).
7. F. Reichert, T. Calmano, S. Müller, D.-T. Marzahl, P. W. Metz, and G. Huber, Opt. Lett. **38**, 2698 (2013).
8. F. Starecki, W. Bolaños, A. Braud, J.-L. Doualan, G. Brasse, A. Benayad, V. Nazabal, B. Xu, R. Moncorgé, and P. Camy, Opt. Lett. **38**, 455 (2013).
9. T. Gün, P. Metz, and G. Huber, Opt. Lett. **36**, 1002 (2011).
10. B. Xu, F. Starecki, D. Paboeuf, P. Camy, J. L. Doualan, Z. P. Cai, A. Braud, R. Moncorgé, P. Goldner, and F. Bretenaker, Opt. Express **21**, 5567 (2013).
11. B. Xu, Z. Liu, H. Xu, Z. Cai, C. Zeng, S. Huang, Y. Yan, F. Wang, P. Camy, J. L. Doualan, A. Braud, and R. Moncorgé, Opt. Commun. **305**, 96 (2013).
12. Y. Shi, C. V. Poulsen, M. Sejka, and O. Poulsen, J. Lightwave Technol. **12**, 749 (1994).
13. S. Ruan, B. H. T. Chai, J. M. Sutherland, P. M. W. French, and J. R. Taylor, Opt. Lett. **20**, 1041 (1995).
14. Y. P. Tong, A. V. Shestakov, B. H. T. Chai, J. M. Sutherland, P. M. W. French, and J. R. Taylor, Opt. Lett. **21**, 644 (1996).
15. J. M. Sutherland, B. H. T. Chai, P. M. W. French, and J. R. Taylor, Opt. Lett. **21**, 797 (1996).
16. R. Abe, J. Kojou, K. Masuda, and F. Kannari, Appl. Phys. Express **6**, 032703 (2013).
17. R. Bek, H. Kahle, T. Schwarzbäck, M. Jetter, and P. Michler, Appl. Phys. Lett. **103**, 242101 (2013).
18. S. Ranta, A. Härkönen, T. Leinonen, L. Orsila, J. Lyytikäinen, G. Steinmeyer, and M. Guina, Opt. Lett. **38**, 2289 (2013).